MHD CONVECTIVE FLOW PAST A VERTICAL POROUS PLATE UNDER THE INFLUENCE OF THERMAL AND MASS DIFFUSION

¹ N. SWAMY KALLEPALLI^{, 2} Ch. V. RAMANA MURTHY, &
³ K. JHANSI RANI

¹Department of Mathematics, Sri Vasavi Institute of Engineering & Technology, Nandamuru- 521369 (A.P) INDIA

²Department of Mathematics, Koneru Lakshmaiah Education Foundation, Vaddeswaram - 522502 (A. P) INDIA

³ Freshman Engineering Department, Lakireddy Balireddy College of Engineering, Mylavaram -521230(A.P) INDIA

Abstract

The aim or the present analysis is to provide a visual representation of the results of an analysis of the effects of temperature and mass diffusion on MHD convective flow through a vertical porous plate. The nature of velocity in respect to the many important factors appearing in the field equations was not discussed at length. It is also shown that the boundary surface plays a crucial role in the uniform suction. It is shown that the velocity decreases with an increase in the Prandtl number. When the fluid reaches the boundary layer, it reverses direction and continues to move ahead. As the Prandtl number increases, it is shown that velocities must fall. There is evidence of forward movement of the fluid after a brief period of reverse flow toward the boundary layer. Additionally, as the Grashoff number rises, so does the velocity of the fluid. When this occurs, progress temporarily halts before picking up again. The apparent velocity then increases when the pore size is increased. In general, speeds increase as pore diameters become smaller. Here, we have a predominance of reverse flow, followed by forward motion due to the predominance of fluid velocity. There is a strong correlation between the Prandtl number and the flow rate.

1. Nomenclature

A	Suction parameter
С	Dimensionless species concentration
C_r	Specific heat at constant pressure
C^*	Species concentration
C_w^*	Concentration at the wall
C.*	Concentration in free stream
D	Molecular diffusivity of the species
g	Gravity
Gc	Modified Grashoff number
Gr	Grashof number
h	Rarefaction parameter
k	Thermal conductivity
K	Dimensionless Permeability parameter
K^*	Permeability parameter
L^*	Constant
M	Magnetic intensity
P_r	Prandtl number
q_w^*	Heat flux at the wall
Sc	Schmidt number
t	Dimensionless time
t^*	Time
T^*	Temperature
T_w^*	Temperature of wall
T_{∞}^*	Temperature of fluid in free stream
и	Dimensionless velocity component
u*	Velocity component
V	Suction velocity
V ₀ *	Constant mean suction velocity

2. Greek Symbols

α : Thermal diffusivity

B: Coefficient of thermal expansion

 β_0 : Coefficient of thermal expansion with concentration

€ : Amplitude (<<1)

Viscosity

v : Kinematic viscosity

θ : Dimensionless temperature

p : Density

Stefan-Boltzmann constant

T: Dimensionless shearing stress

τ* : Shearing stress

w : Dimensionless frequency

w*: Frequency

3. Introduction

There are several commercial and ecological settings where radiative convective flow is crucial. Applications are most common in areas including solar energy, space exploration, energy efficiency, and cooling systems. The idea is mostly used to the optimization and design of high-precision machinery seen in nuclear power plants, aircraft propulsion systems, and gas turbines.

Stokes was the first to investigate the issue of a viscous incompressible fluid on an endless horizontal plate flowing in its own plane. Since then, Brinkman [2] has studied the influence of viscosity on dense particles in fluid. In subsequent work, Stewartson [3] looked into the analytical solution for a viscous flow across a semiinfinite horizontal plate. Next, Berman [4] looked into the impact of uniform suction or injection on the constant flow of an incompressible fluid through porous barriers in two dimensions. On the premise that the wall temperature changes linearly in the direction of flow, Mori [5] subsequently investigated the current between two nonconducting vertical plates. In continuation of this work, Macy [6] studied the dynamics of flow in renal tubes with a constant cross section, permeable border, and a radial velocity that changes as an exponentially decreasing function. Hall [7] investigated a similar issue by employing the finite differences approach to ensure the stability of the solution. After that, Mahajan et al. [8] looked at how natural convective flows are affected by the viscous heat dissipation effect. A further study by Soundalgekar and Thaker [9] looked at the impact of heat radiation on very thin gray gas confined inside a vertically fixed plate. Later, Hossain et al. [10] used Rossland's technique to investigate how radiation affects a vertical plate maintained at a fixed

surface temperature. Raptis and Perdikis [11] revealed the results of a computational study of the effect of heat radiation and convective flow through an infinite vertically moving plate. Later, Antony Raj [12] studied the impact of a transversely applied magnetic field on the flow through a semi-infinite vertical isothermal plate subject to a homogenous heat flux due to thermal radiation.

It is quite apt and reasonable to state that, Tessone et al. [13] focused on the Dufour and Soret effects on free convection and mass exchange using a rotating model with a semi-endless, vertical plate to see more about consistent MHD mass exchange through porous medium. Electric conducting fluid flows between two indefinitely long horizontal porous flats in a three-dimensional couette motion. Subsequently Motsa [14] employed a novel method to study he MHD effects on the fluid flow. Thereafter Khan [15] examined "Peristaltic transport of a Jeffrey fluid with variable viscosity through a porous medium in an asymmetric channel. An unsteady MHD convective flow across an indefinitely porous sliding porous plate was explored in this paper by Ellahi et al. [16]. Heat and mass transmission across a constantly changing porous barrier were studied by Umar et al. [17] in the applied magnetic field. MHD viscous flow across an infinite vertical plate with a continuous mass flux was studied by Ramesh et al. [18]. Even if the governing equations are difficult, making the correct assumptions can make them easier to understand. Many scholars have studied the Hall effect on MHD free and induced mixed convection in a rotating porous channel. In a non-uniform horizontal circular cylinder, Ramzan et al. [19] looked at convective flow in practical situations. The incompressible and insulating material according to Mohamed et al. [20] Under an angled magnetic field, the Williamson fluid moved peristaltically in a planar channel with heat and mass transfer. Magnetic fields were applied to porous media in order to study the flow of two stress fluids when the walls slipped. There was a discussion on theoretical and computational assessments. Numerical study of magnetic effect on the velocity distribution field in a macro/microscale of a micropolar and viscous fluid in vertical channel was analysed by Tetbirt et al [21]. Using an elastic and viscous deformation fluid, Ghadikolaei et al. [22] found that a sliding vertical plate with time-dependent velocity, which was in the vicinity of the porous medium, produced erratic MHD flow. Magnetohydrodynamic natural circulation flow in a rotating media is crucial to understand since it has applications in a variety of domains, including astronomy, geophysics, and fluid engineering. Flowfield occurs when the density of an incompressible viscous fluid is low or when a strong magnetic field is applied. Since the Hall current causes second-order flow, it is a crucial tool for determining the flow properties of problems.

The afore mentioned works omitted thorough commentary on the nature of velocity in relation to the important quantities which exist in the field equations. In addition, the relevance of the bounded surface with regard to the uniform suction or injection was not investigated.

4. Mathematical Model

Slip-flow regime is discussed in this chapter, which describes the flow of a viscous, incompressible fluid through a vertically porous, infinitely thin flat plate that is susceptible to shear. The suction velocity distribution is not uniform when temperature and concentration are periodically changing. V^* $V_0^*(1+\varepsilon Ae^{iw^*t})$

fluctuating with respect to time is considered. A rectangular Cartesian co-ordinate

system with wall lying vertically in x^*y^* -plane is employed. The axis is taken in vertically upward direction along the vertical porous plate and y^* -axis is taken normal to the plate.

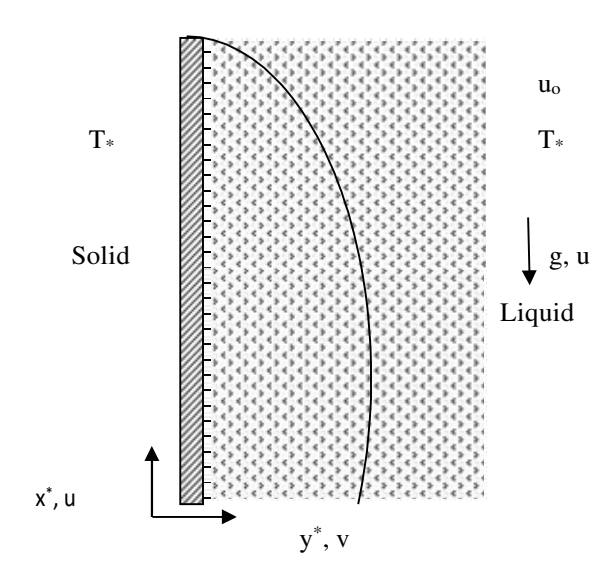


Figure: Schematic representation of the problem

Since the plate is considered infinite in the x^* -direction, hence all physical quantities will be independent of x^* . In this setting, y^* and t^* are the only independent variables in the physical variables. If viscous dissipation is ignored and density variation is assumed in the body force component (Boussinesq's approximation), then the following set of equations may be used to solve the problem.

$$\frac{\partial u^*}{\partial t^*} - V_0^* \left(1 + \varepsilon A e^{i v \cdot t^*} \right) \frac{\partial u^*}{\partial y^*} = g \beta (T^* - T_\infty^*) + g \beta^0 (C^* - C_\infty^*) + v \frac{\partial^2 u^*}{\partial y^{*2}} - \frac{\sigma \beta_0^2}{\rho} u^* - \frac{v}{R^*} u^*$$
(1)

$$\rho C_p \left[\frac{\partial T^*}{\partial t^*} - V_0^* \left(1 + \varepsilon A e^{iw^* t^*} \right) \frac{\partial T^*}{\partial y^*} \right] = k \frac{\partial^2 T^*}{\partial y^{*2}}$$
 (2)

$$\frac{\partial c^*}{\partial t^*} - V_0^* \left(1 + \varepsilon A e^{i v^* t^*} \right) \frac{\partial c^*}{\partial v^*} = D \frac{\partial^2 c^*}{\partial v^{*2}}$$
 (3)

The boundary conditions of the problem are:

$$u^{*} = L^{*} \left(\frac{\partial u^{*}}{\partial y^{*}} \right), T^{*} = T_{w}^{*} + \varepsilon (T_{w}^{*} - T_{\infty}^{*}) e^{iw^{*}t^{*}}, C^{*} = C_{w}^{*} + \varepsilon (C_{w}^{*} - C_{\infty}^{*}) e^{iw^{*}t^{*}} \text{ at } y^{*} = 0$$

$$u^{*} \to 0, T^{*} \to T_{\infty}^{*}, C^{*} \to C_{\infty}^{*} \text{ as } y^{*} \to \infty$$

$$(4)$$

These new dimensions are introduced into equations as follows

$$y = \frac{y^*V_0^*}{v}, t = \frac{t^*V_c^{*2}}{4v}, u = \frac{4vw^*}{V_0^{*2}}, \theta = \frac{T^* - T_\infty^*}{T_w^* - T_w^*}, C = \frac{C^* - C_\infty^*}{C_w^* - C_\infty^*}, Gr = \frac{g\beta v(T^* - T_\infty^*)}{V_0^{*3}}.$$

$$Gc = \frac{g\beta v(C_w^* - C_\infty^*)}{V_0^{*3}}, Pr = \frac{\mu C_p}{k} = \frac{v\rho C_p}{k}, Sc = \frac{v}{D}, K = \frac{K^*V_0^{*2}}{v^2}, h = \frac{V_0^*L^4}{v}$$

All physical variables are defined in nomenclature where (*) indicates the dimensional quantities. The subscript (*) denotes the free stream condition. Then equations (1) to (3) reduce to the following non-dimensional form:

$$\frac{1}{4}\frac{\partial u}{\partial t} - \left(1 + \varepsilon A e^{iwt}\right)\frac{\partial u}{\partial y} = Gr\theta + GcC + \frac{\partial^2 u}{\partial y^2} - \frac{u}{k}$$
 (5)

$$\frac{1}{4}\frac{\partial\theta}{\partial z} - \left(1 + \varepsilon A e^{iwt}\right) \frac{\partial\theta}{\partial y} = \frac{1}{Pr} \frac{\partial^2\theta}{\partial y^2} \tag{6}$$

In the dimensionless version, the problem's boundary conditions are as follows:

$$u = h\left(\frac{\partial u}{\partial y}\right), \theta = 1 + \varepsilon e^{iwt} \quad \text{at } y = \mathbf{0}$$

$$u \to 0, \quad \theta \to 0, \qquad \text{as } y \to \infty$$

$$(7)$$

5. Method of Solution:

Assuming the small amplitude oscillations ($\varepsilon \ll 1$), we can represent the velocity u, temperature θ and concentration C near the plate as follows:

$$u(y,t) = u_0(y)e^{iwt}$$
(8)

$$\theta(y,t) = \theta_0(y)e^{iwt} \tag{9}$$

Substituting (8) to (9) in (5) to (6), equating the coefficients of non-harmonic terms and neglecting of ϵ^{\ddagger} on both sides

$$u_0 + u_0 - \left(\frac{1}{R} + \frac{tw}{4}\right)u_0 = -Gr\theta_0 - GcC_0 - Au_0 \tag{10}$$

$$\theta_0^* + Pr\theta_0^* \quad \frac{twPr}{4} \ell_0 = -A\theta_0^* Pr \tag{11}$$

Together, these boundary conditions boil down to:

$$u_0 = 0$$
 , $\frac{\partial u_0}{\partial y} - 0$ at $y = 0$, $\theta_0 = 1$, $\frac{\partial \theta_0}{\partial y} - 0$ at $y = 0$ (12)

Where y-differentiation is denoted by primes. After plugging in the boundary conditions (12), we may solve equations (10) and (11), yielding:

$$u_{0}(y) = c_{1}e^{m_{1}y} + c_{2}e^{m_{2}y} + \frac{Gr\theta_{0} + GcC_{0}}{\left(\frac{1}{K} + \frac{iw}{4}\right)}$$
(13)

$$\theta_0(y) = c_3 e^{m_a y} + c_4 e^{m_4 y} \tag{14}$$

Where

$$m_1 = \frac{-(1+A) + \sqrt{(1+A)^2 + 4(\frac{1}{K} + \frac{\dot{n}v}{4})}}{2}, m_2 = \frac{-(1+A) - \sqrt{(1+A)^2 + 4(\frac{1}{K} + \frac{\dot{n}v}{4})}}{2}, \ c_1 = \frac{m_2}{m_1 - m_2}, \frac{Gr\theta_0 + GcC_0}{\left(\frac{1}{K} + \frac{\dot{n}v}{4}\right)}, \ c_2 = \frac{-(1+A) - \sqrt{(1+A)^2 + 4(\frac{1}{K} + \frac{\dot{n}v}{4})}}{2}, \ c_3 = \frac{m_2}{m_1 - m_2}, \frac{Gr\theta_0 + GcC_0}{\left(\frac{1}{K} + \frac{\dot{n}v}{4}\right)}, \ c_4 = \frac{m_2}{m_1 - m_2}, \frac{Gr\theta_0 + GcC_0}{\left(\frac{1}{K} + \frac{\dot{n}v}{4}\right)}, \ c_5 = \frac{m_2}{m_1 - m_2}, \frac{Gr\theta_0 + GcC_0}{\left(\frac{1}{K} + \frac{\dot{n}v}{4}\right)}, \ c_7 = \frac{m_2}{m_1 - m_2}, \frac{Gr\theta_0 + GcC_0}{\left(\frac{1}{K} + \frac{\dot{n}v}{4}\right)}, \ c_7 = \frac{m_2}{m_1 - m_2}, \frac{Gr\theta_0 + GcC_0}{\left(\frac{1}{K} + \frac{\dot{n}v}{4}\right)}, \ c_7 = \frac{m_2}{m_1 - m_2}, \frac{Gr\theta_0 + GcC_0}{\left(\frac{1}{K} + \frac{\dot{n}v}{4}\right)}, \ c_7 = \frac{m_2}{m_1 - m_2}, \frac{Gr\theta_0 + GcC_0}{\left(\frac{1}{K} + \frac{\dot{n}v}{4}\right)}, \ c_7 = \frac{m_2}{m_1 - m_2}, \frac{Gr\theta_0 + GcC_0}{\left(\frac{1}{K} + \frac{\dot{n}v}{4}\right)}, \ c_7 = \frac{m_2}{m_1 - m_2}, \frac{Gr\theta_0 + GcC_0}{\left(\frac{1}{K} + \frac{\dot{n}v}{4}\right)}, \ c_7 = \frac{m_2}{m_1 - m_2}, \frac{Gr\theta_0 + GcC_0}{\left(\frac{1}{K} + \frac{\dot{n}v}{4}\right)}, \ c_7 = \frac{m_2}{m_1 - m_2}, \frac{Gr\theta_0 + GcC_0}{\left(\frac{1}{K} + \frac{\dot{n}v}{4}\right)}, \ c_7 = \frac{m_2}{m_1 - m_2}, \frac{Gr\theta_0 + GcC_0}{\left(\frac{1}{K} + \frac{\dot{n}v}{4}\right)}, \ c_7 = \frac{m_2}{m_1 - m_2}, \frac{Gr\theta_0 + GcC_0}{\left(\frac{1}{K} + \frac{\dot{n}v}{4}\right)}, \ c_7 = \frac{m_2}{m_1 - m_2}, \frac{Gr\theta_0 + GcC_0}{\left(\frac{1}{K} + \frac{\dot{n}v}{4}\right)}, \ c_7 = \frac{m_2}{m_1 - m_2}, \frac{Gr\theta_0 + GcC_0}{\left(\frac{1}{K} + \frac{\dot{n}v}{4}\right)}, \ c_7 = \frac{m_2}{m_1 - m_2}, \frac{Gr\theta_0 + GcC_0}{\left(\frac{1}{K} + \frac{\dot{n}v}{4}\right)}, \ c_7 = \frac{m_2}{m_1 - m_2}, \frac{Gr\theta_0 + GcC_0}{\left(\frac{1}{K} + \frac{\dot{n}v}{4}\right)}, \ c_7 = \frac{m_2}{m_1 - m_2}, \frac{Gr\theta_0 + GcC_0}{\left(\frac{1}{K} + \frac{\dot{n}v}{4}\right)}, \ c_7 = \frac{m_2}{m_1 - m_2}, \frac{Gr\theta_0 + GcC_0}{\left(\frac{1}{K} + \frac{\dot{n}v}{4}\right)}, \ c_7 = \frac{m_2}{m_1 - m_2}, \frac{Gr\theta_0 + GcC_0}{\left(\frac{1}{K} + \frac{\dot{n}v}{4}\right)}, \ c_7 = \frac{m_2}{m_1 - m_2}, \frac{Gr\theta_0 + GcC_0}{\left(\frac{1}{K} + \frac{\dot{n}v}{4}\right)}, \ c_7 = \frac{m_2}{m_1 - m_2}, \frac{Gr\theta_0 + GcC_0}{\left(\frac{1}{K} + \frac{\dot{n}v}{4}\right)}, \ c_7 = \frac{m_2}{m_1 - m_2}, \frac{Gr\theta_0 + GcC_0}{\left(\frac{1}{K} + \frac{\dot{n}v}{4}\right)}, \ c_7 = \frac{m_2}{m_1 - m_2}, \frac{Gr\theta_0 + GcC_0}{\left(\frac{1}{K} + \frac{\dot{n}v}{4}\right)}, \ c_7 = \frac{m_2}{m_1 - m_2}, \frac{Gr\theta_0 + GcC_0}{\left(\frac{1}{K} + \frac{\dot{n}$$

$$\begin{split} c_2 &= \frac{m_4}{m_4 - m_2} \cdot \frac{Gr \, \theta_0 \, \| \, \theta \, e \, \theta_0}{\left(\frac{1}{K} + \frac{iw}{4}\right)} \, , \\ m_{\rm E} &= \frac{-\left(1 + A\right) p_T + \sqrt{\left(p_T \left(1 + A\right)\right)^2 + iw p_T}}{2} \, , \\ m_4 &= \frac{-\left(1 + A\right) p_T - \sqrt{\left(p_T \left(1 + A\right)\right)^2 + iw p_T}}{2} \end{split} ,$$

$$c_3 = \frac{-m_4}{m_3 - m_4}, c_4 = \frac{m_3}{m_3 - m_4}$$

6. Results:

1. The impact of the Prandtl number on the velocity profiles for Gr = 18 and Gr = 24 are shown in Figures 1 and 2, respectively. In all of these examples, the velocity drops down noticeably as the Prandtl number rises. Fluid motion is also shown to be forward after a brief period of backward flow close to the boundary layer.

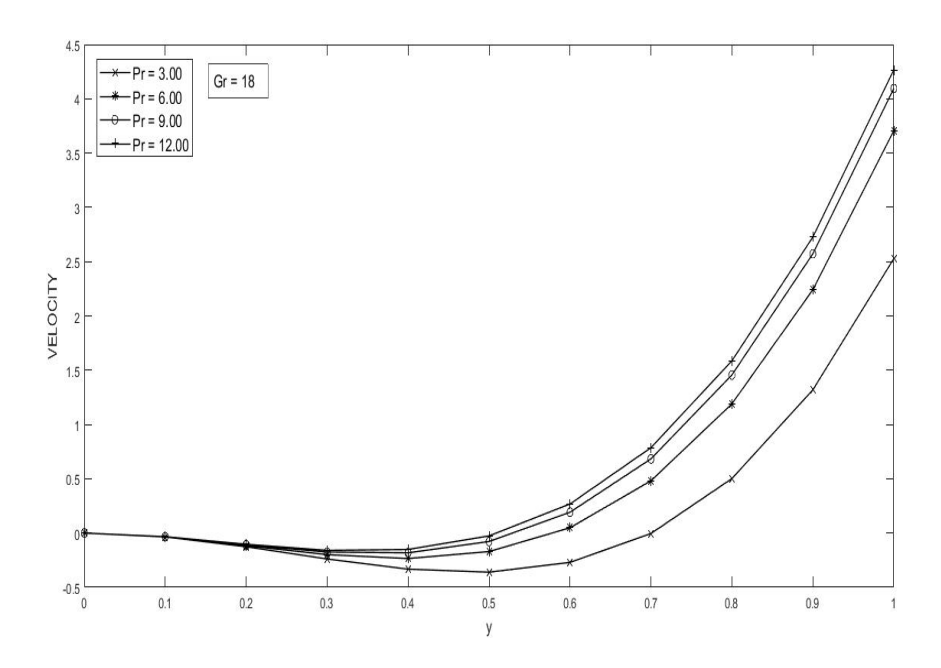


Figure-1: Variation of Velocity profiles w.r.t Prandtl number for Gr = 18

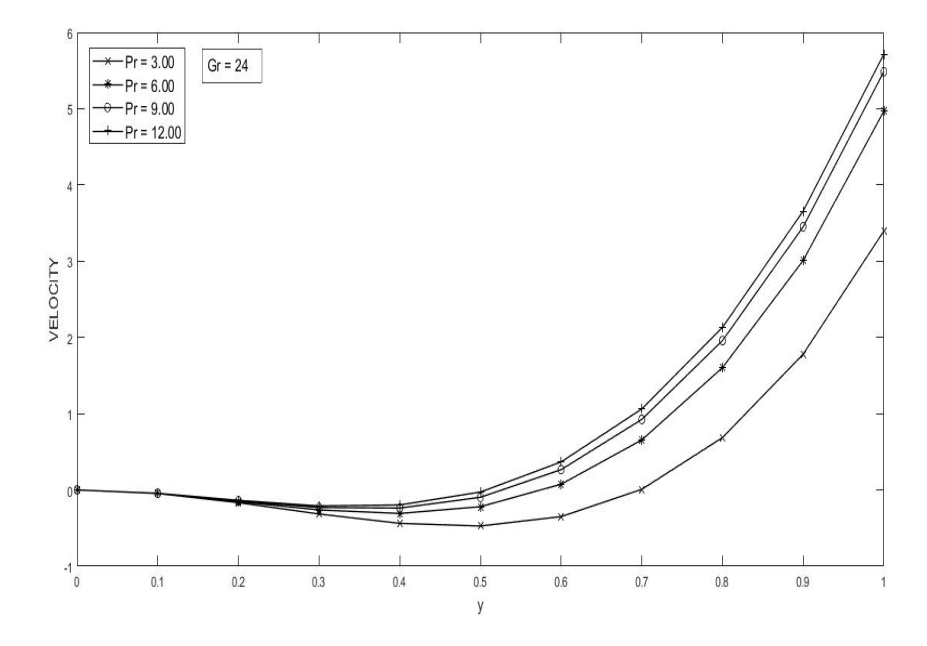


Figure-2: Nature of Velocity profiles for Gr = 24

2. Figures 3, 4, and 5 depict three different velocity patterns for a given Prandtl number. The velocity of the fluid is found to grow according to the Grashoff number. In this situation, too, there is a brief period of reverse motion followed by forward movement.

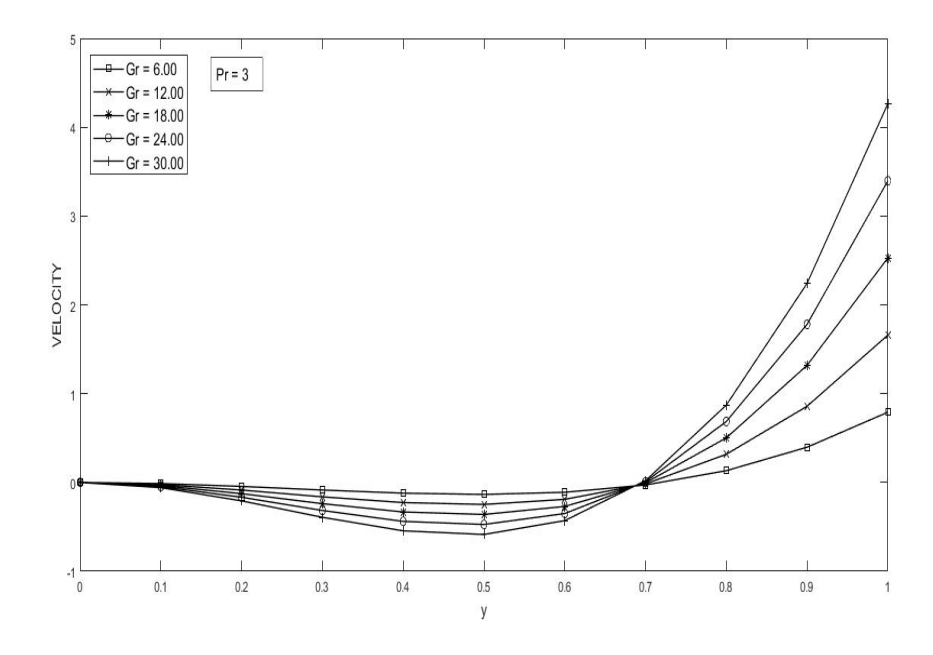


Figure-3: Influence of Grashoff number on Velocity profiles for Pr = 3

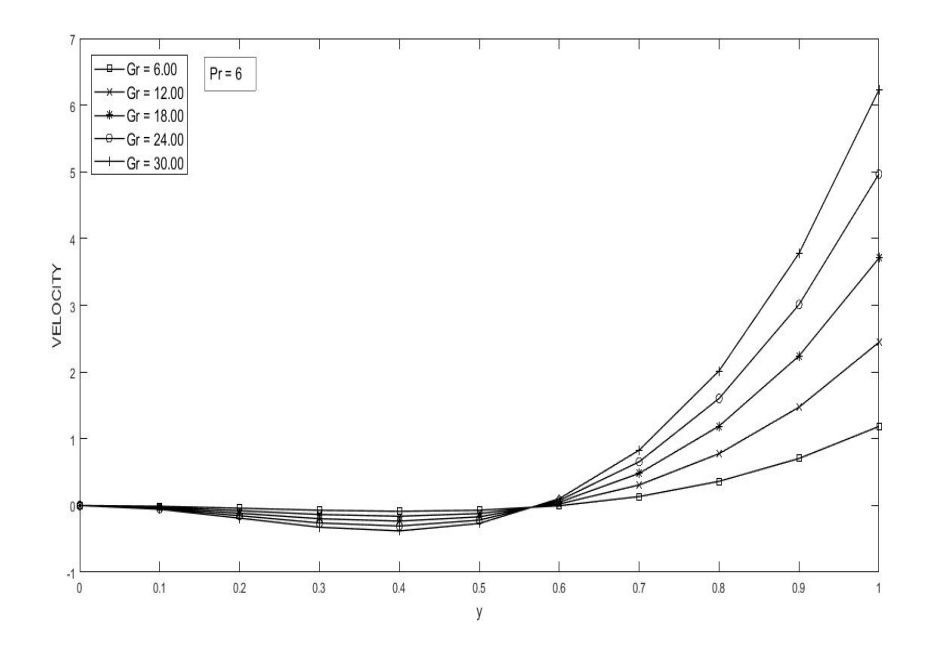


Figure-4: Variation of Velocity profiles w.r.t Grashoff number for Pr = 6

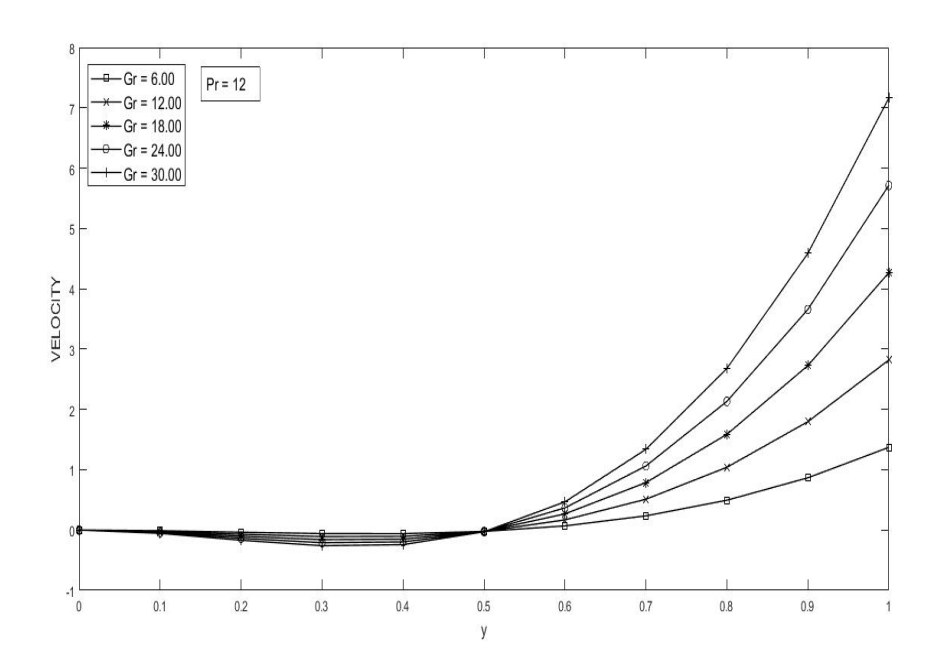


Figure-5: Effect of Grashoff number on Velocity profiles for Pr = 12

3. Figure 6 depicts the influence of porosity when the Prandtl number is held constant. The velocity seems to be growing as the pore size grows.

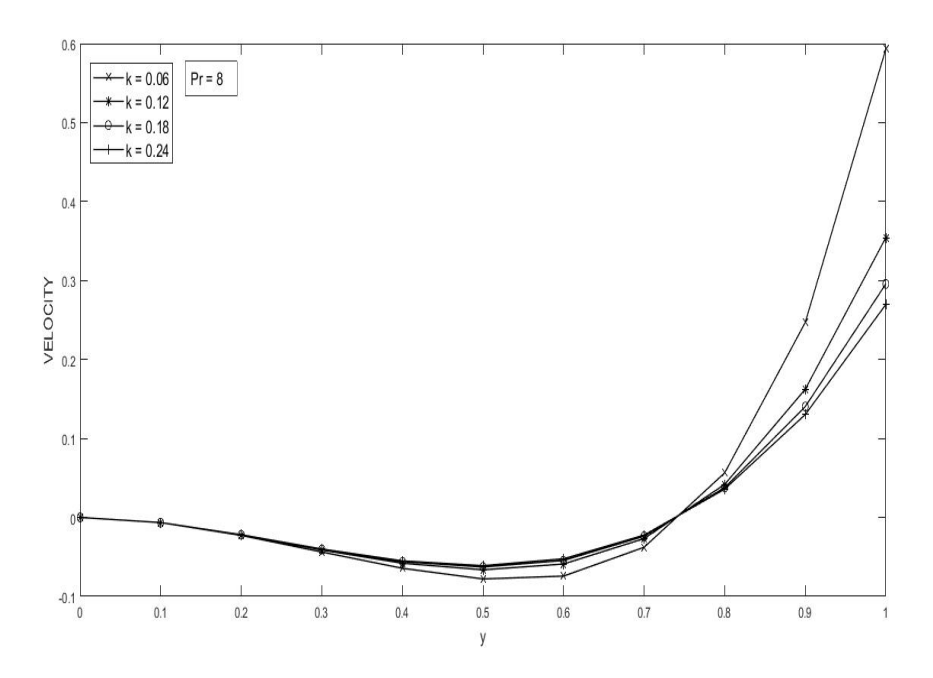


Figure-6: Variation of Velocity profiles w.r.t Porosity for Pr = 8

4. The results of varying the Prandtl number are shown in the velocity profiles in Figures 7, 8, and 9 for k = 0.06, k = 0.12, and k = 0.24. In every case, it has been shown that the velocity rises along with the pore size. Here, we have a predominance of reverse flow, followed by forward motion due to the predominance of fluid velocity.

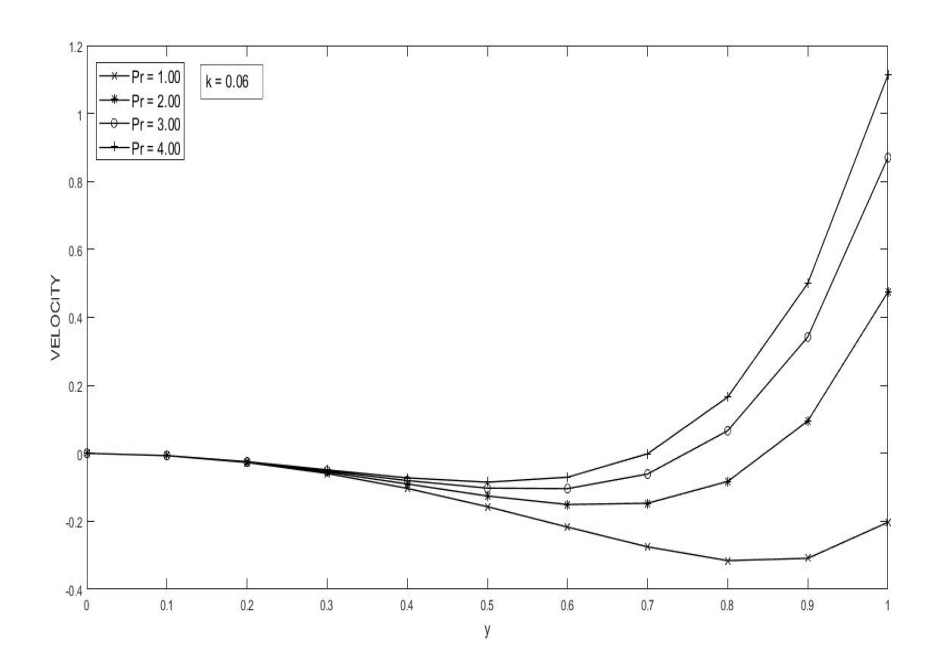


Figure-7: Nature of Velocity profiles for k = 0.06

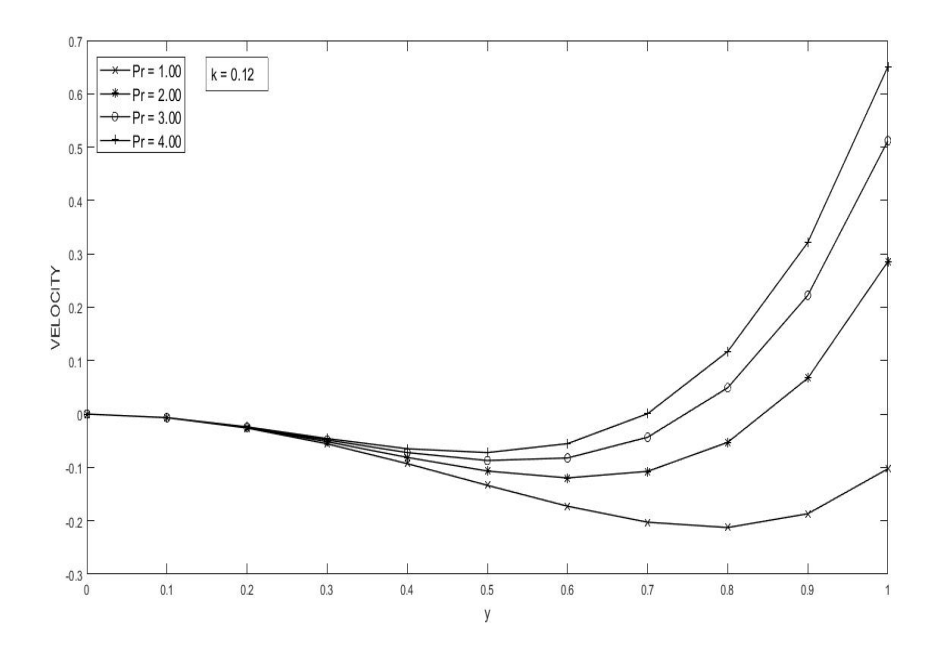


Figure-8: Effect of Prandtl number on Velocity profiles for k = 0.12

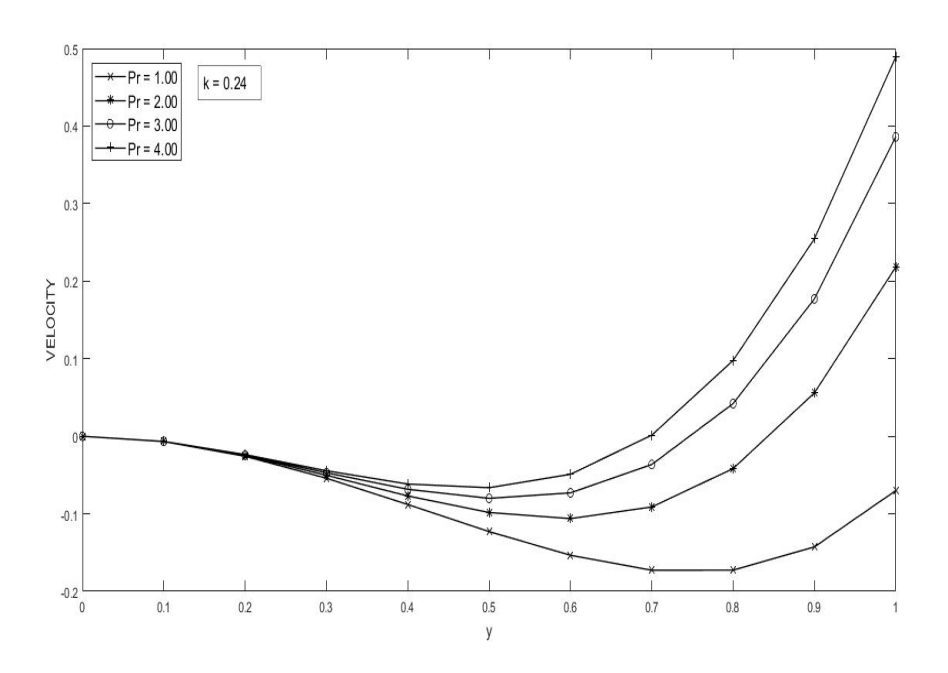


Figure-9: Influence of Prandtl number on Velocity profiles for k = 0.24

5. Figures 10 and 11 illustrate the relationship between the Prandtl number and the flow rate for a constant pore size. An increasing rate of flow is seen to correspond to an increasing Prandtl number.

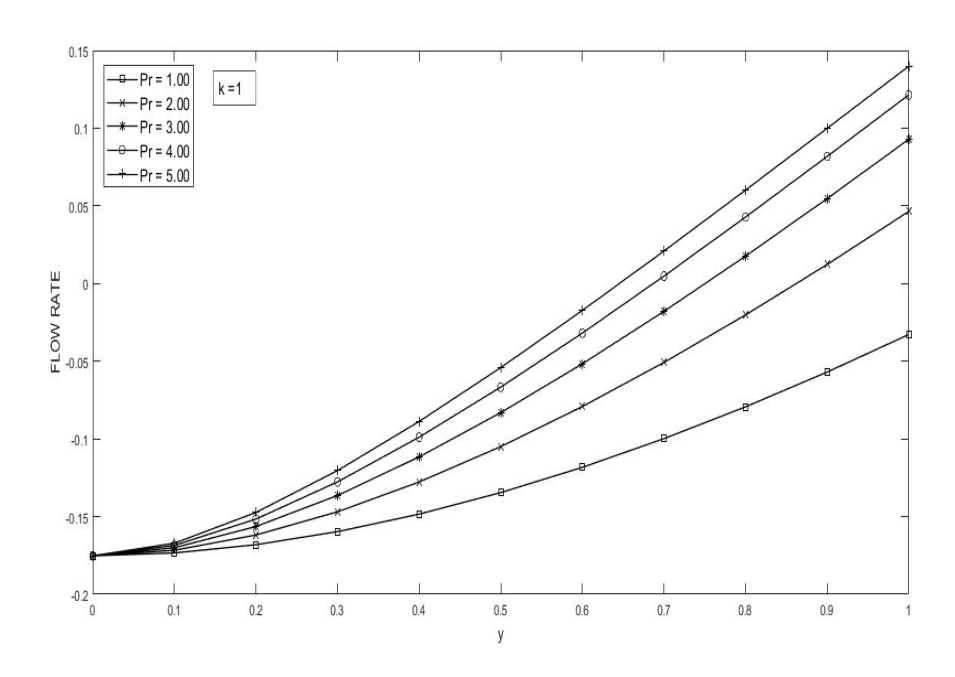


Figure-10: Nature of Flow rate w.r.t Prandtl number for k = 1

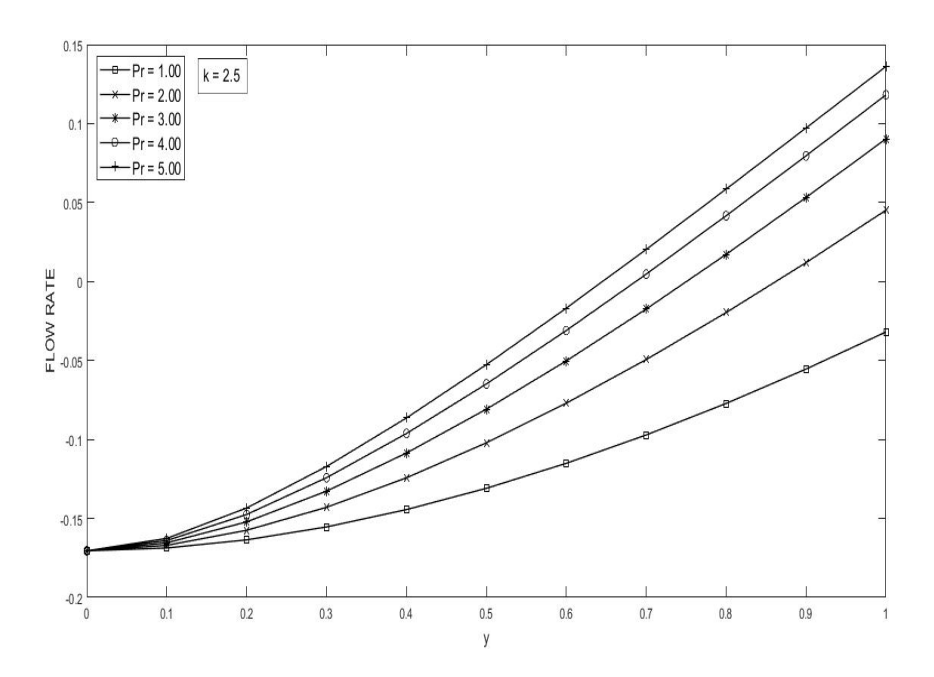


Figure-11: Variation of Flow rate w.r.t Prandtl number for k = 2.5

6. Figures 12 and 13 show how the flow rate changes when the porosity of the fluid bed is altered while the Prandtl number remains constant. The flow rate increases with increasing porosity, as seen by these many instances. The Prandtl number is highly correlated with the velocity of a fluid.

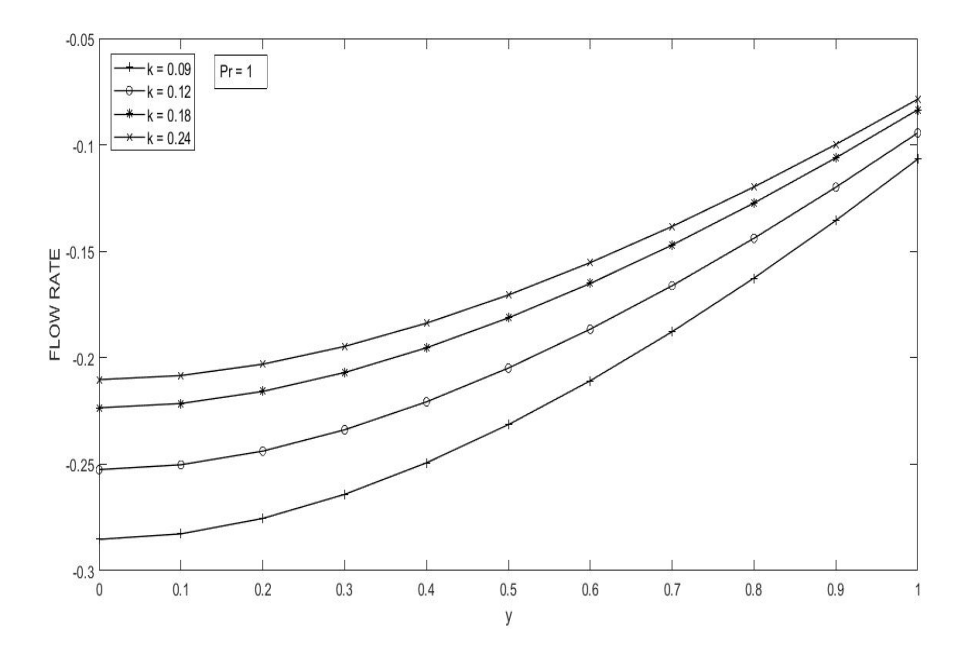


Figure-12: Nature of Flow rate w.r.t Porosity for Pr = 1

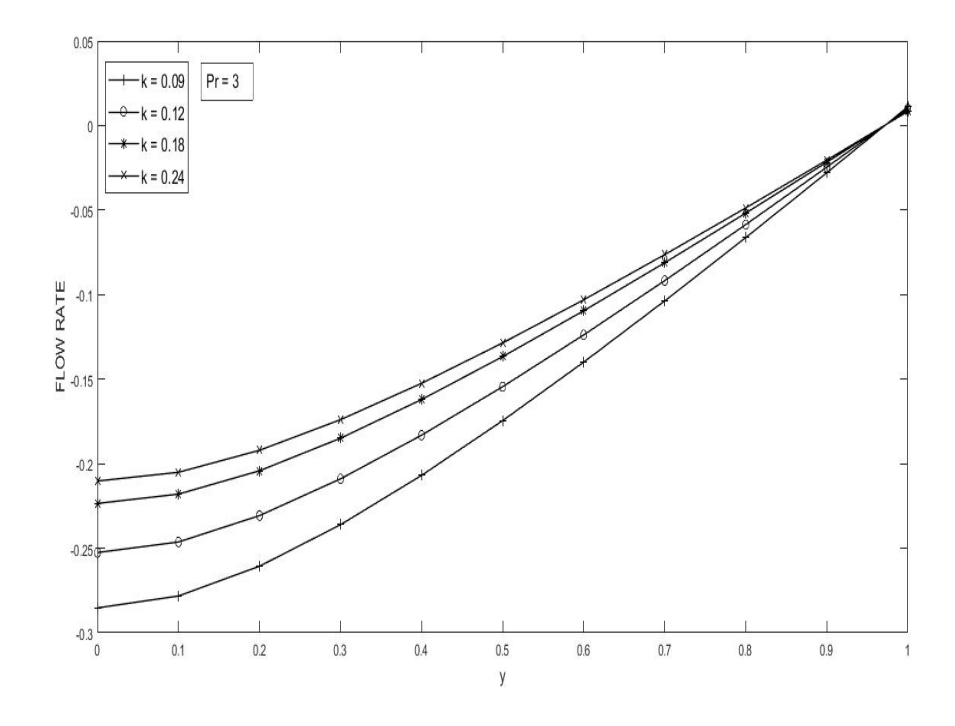


Figure-13: Effect of Porosity on Flow rate for Pr = 3

7. Conclusions:

When the Grashoff parameter is held constant the velocity drops down noticeably as the Prandtl number rises. Fluid motion is also shown to be forward after a brief period of backward flow close to the boundary layer. Subsequently, for a given Prandtl number the velocity of the fluid is found to grow according to the Grashoff number. For a brief period of reverse motion followed by forward movement. Also, the velocity seems to be growing as the pore size grows. An increasing rate of flow is seen to correspond to an increasing Prandtl number. Also, the flow rate increases with increasing porosity, as seen by these many instances. The Prandtl number is highly correlated with the velocity of a fluid.

References

- 1. Stokes. G.G On the effects of Internal Friction of fluids on the Motion of Pendulums, *Camb.Phil. Trans IX*, 2, Pp. 8 106. (1851).
- 2. Brinkman H.C, A calculation of viscous force extended by flowing fluid in a dense swarm of particles. *Appl.sci.Res*, *A* (1) Pp 27 34 (1947).
- 3. Stewartson. K., On the impulsive Motion of a Flat plate in a Viscous Fluid. *Quarterly Jnl. Of Mechanics and Applied Mathematics, IV*, 2, Pp. 182 198, (1951).
- 4. Berman. A. S. Laminer flow in a channel with porous walls *Jnl. Appl.Phys*, 24, Pp. 1232 1235, (1953).
- 5. Mori Y, On combined free and forced convective laminar MHD flow and heat transfer in channels with transverse magnetic field, international developments in heat transfer, ASME paper no.124, Pp 1031 1037(1961).
- 6. Macey R.I., Pressure flow patterns in a cylinder with reabsorbing wall, *Bull Math Biophys*, 25(1), (1963).
- 7. Hall. M. G. The Boundary layer over an impulsively started flat plate, *Proc. Roy. Soc. A.*310,1502, Pp. 401 414, (1969).
- 8. Mahajan R. L., Gebhart. B.B., Viscous Dissipation Effects in Buoyancy Induced flows., *Int. Jnl, of Heat Mass Transfer*, 32, 7, Pp. 1380 1382, (1989).

- Soundalgekar V. M. and Thaker H.S.: Radiation effects on free convection flow past a semi-infinite vertical plate *Modeling measurement and control*, vol. B51, Pp 31 40, (1993).
- 10. Hossain M. A. and Takhar, Radiation effect on mixed convection along a vertical plate with uniform surface temperature, *Heat and Mass Transfer*, 31, Pp 243 248, (1996).
- 11. Raptis. A and Perdikis C.: Radiation and free convection flow past a moving plate, *Int. J. App. Mech. Engg*, 4, 817 821, (1999).
- 12. Chandrakala P and Antony Raj S: Radiation effects on MHD flow past an impulsively started vertical plate with uniform heat flux, *Indian Journal of Mathematics*, 50 (3), 519 532, (2008).
- 13. A. Tassone, G. Caruso, F. Giannetti, and A. D. Nevo, "MHD mixed convection flow in the WCLL: heat transfer analysis and cooling system optimization," Fusion Engineering and Design, vol. 146, pp. 809–813, 2019. View at: Publisher Site | Google Scholar
- 14. S. S. Motsa, P. G. Dlamini, and M. Khumalo, "Spectral relaxation method and spectral quasilinearization method for solving unsteady boundary layer flow problems," Advances in Mathematical Physics, vol. 2014, Article ID 341964, 12 pages, 2014. View at: Publisher Site | Google Scholar
- 15. A. A. Khan, R. Ellahi, and K. Vafai, "Peristaltic transport of a Jeffrey fluid with variable viscosity through a porous medium in an asymmetric channel," Advances in Mathematical Physics, vol. 2012, Article ID 169642, 15 pages, 2012. View at: Publisher Site | Google Scholar
- **16.** R. Ellahi, "A study on the convergence of series solution of non-Newtonian third grade fluid with variable viscosity by means of homotopy analysis method," Advances in Mathematical Physics, vol. 2012, Article ID 634925, 11 pages, 2012. View at: Publisher Site | Google Scholar
- 17. M. Umar, R. Akhtar, Z. Sabir et al., "Numerical treatment for the three-dimensional Eyring-Powell fluid flow over a stretching sheet with velocity slip and activation energy," Advances in Mathematical Physics, vol. 2019, Article ID 9860471, 12 pages, 2019. View at: Publisher Site | Google Scholar
- **18.** G. K. Ramesh, B. J. Gireesha, and C. S. Bagewadi, "Heat transfer in MHD dusty boundary layer flow over an inclined stretching sheet with non-

uniform heat source/sink," Advances in Mathematical Physics, vol. 2012, Article ID 657805, 13 pages, 2012. View at: Publisher Site | Google Scholar

- 19. M. Ramzan, M. Farooq, T. Hayat, and J. D. Chunge, "Radiative and Joule heating effects in the MHD flow of a micropolar fluid with partial slip and convective boundary condition," Journal of Molecular Liquids, vol. 221, pp. 394–400, 2016. View at: Publisher Site | Google Scholar
- **20.** R. A. Mohamed, S. M. Abo-Dahab, and T. A. Nofal, "Thermal radiation and MHD effects on free convective flow of a polar fluid through a porous medium in the presence of internal heat generation and chemical reaction," Mathematical Problems in Engineering, vol. 2010, pp. 1–27, 2010. View at: Publisher Site | Google Scholar
- 21. A. Tetbirt, M. N. Bouaziz, and M. T. Abbes, "Numerical study of magnetic effect on the velocity distribution field in a macro/micro-scale of a micropolar and viscous fluid in vertical channel," Journal of Molecular Liquids, vol. 216, pp. 103–110, 2016. View at: Publisher Site | Google Scholar
- 22. S. S. Ghadikolaei, K. Hosseinzadeh, and D. D. Ganjib, "Numerical study on magnetohydrodynic CNTs-water nanofluids as a micropolar dusty fluid influenced by non-linear thermal radiation and Joule heating effect," Powder Technology, vol. 340, pp. 389–399, 2018. View at: Publisher Site | Google Scholar